DOI: 10.17725/rensit.2023.15.415

Generation and detection of spin current in iridate/manganite heterostructure

Georgy D. Ulev, Gennady A. Ovsyannikov, Karen Y. Constantinian, Anton V. Shadrin, Ivan E. Moscal, Peter V. Lega

Kotel'nikov Institute of Radioengineering and Electronics of Russian Academy of Sciences, http://cplire.ru/
Moscow 125009, Russian Federation

E-mail: gdulev@edu.hse.ru, gena@hitech.cplire.ru, karen@hitech.cplire.ru, shadrinant@mail.ru, moskal@hitech.cplire.ru, lega_peter@list.ru

Received September 03, 2023, peer-reviewed September 10, 2023, accepted September 17, 2023, published December 06, 2023.

Abstract: **The results of experimental studies on spin current at the interface of iridate/manganite heterostructure $SrIrO_3/La_{0.7}Sr_{0.3}MnO_3$ consisted of oxide epitaxial films with nanometer thickness are presented. A pure spin current was induced by microwave irradiation in GHz frequency band under conditions of ferromagnetic resonance. The spin current was detected due to inverse spin-Hall effect measuring the spectral characteristics of charge current arising on electrically conductive $SrIrO_3$ film with strong spin-orbit interaction. The spin-Hall angle, which characterizes the efficiency of spin current conversion to the charge current, was determined by measurements of the angular dependences of spin magnetoresistance of the iridate/manganite interface.**

Keywords: **spin mixing conductance, spin magnetoresistance, spin-orbit interaction, thin film heterostructure, strontium iridate, manganite**

PACS: 75.47.Lx, 75.25.-j, 73.63.−b

Acknowledgments: The research was supported by a grant from the Russian Science Foundation (project No. 23-49-10006).

For citation: Georgy D. Ulev, Gennady A. Ovsyannikov, Karen Y. Constantinian, Anton V. Shadrin, Ivan E. Moscal, Peter V. Lega. Generation and detection of spin current in iridate/manganite heterostructure. *RENSIT: Radioelectronics. Nanosystems. Information Technologies*, 2023, 15(4):415-424e. DOI: 10.17725/rensit.2023.15.414.

Contents

1. INTRODUCTION

Spintronic devices of give opportunities to solve the problem of heating and energy dissipation in microelectronics, since the spin transfer (spin current) does not generate heat. In modern electronic systems the detection and generation of pure spin current (without charge transfer) require completely different approach to the problem and is based on usage of spin current. One of the possible techniques of generation of pure spin current at the ferromagnetic/normal (non-magnetic) metal interface is the precession of ferromagnetic magnetization (F) induced by microwave magnetic field under ferromagnetic resonance (FMR) conditions. The magnitude of the spin current is determined by the amplitude of magnetization precession and the spin-mixing conductance, which in general has both real and imaginary parts. The spin current could be recorded by charge current, induced by the inverse spin-Hall effect (ISHE) in a metal (N) with strong spin-orbit interaction [1-5]. The presence of both the spin-Hall effect (SHE) and the ISHE causes the spin-Hall magnetoresistance (SMR) in F/N heterostructure [6]. Measurement of the SMR angle dependences is a convenient

tool for determination of spin Hall angle θ_{SH}, which characterizes the efficiency of conversion of spin current into the charge current [6-8].

Experimental study of spin current excitation at the FMR (spin pumping) and its registration due to ISHE in F/N structures where carried out in [2,3] using platinum (Pt) as N metal and permalloy (NiFe) as F metal. Structures with N metal deposited on the top of insulating ferromagnet, the iron-yttrium garnet (YIG) were investigated as well [9,10]. It should be noted, mostly N-metal with strong spin-orbit interaction (SOI) was used [10,11].

In the present work, the 5d transition metal oxide $SrIrO_3$ [12,13] was used, which along with the strong SOI exhibits also electron-electron interaction. The combination of these effects leads to non-trivial quantum phases [14] and to the possibility of controlling of magnetic anisotropy [5]. The charge-spin coupling of $SrIrO_3$ been studied in structures with a metallic ferromagnet deposited on the top of $SrIrO_3$: $SrIrO_3$/Py [15,16], and $SrIrO_3$/$Co_{1-x}Tb_x$ [17]. In these works it was shown that an anomalously large spin-Hall angle is caused by the presence of SOI3 in $SrIrO_3$ which induces a curvature of Berry phase [15,16].

The usage of oxide materials allows to realize heterostructures with atomically smooth interface in the case of growth of thin epitaxial film of strontium iridate $SrIrO_3$ over the epitaxial film $La_{0.7}Sr_{0.3}MnO_3$, grown on $(LaAlO_3)_{0.3}(Sr_2AlTaO_6)_{0.7}$ (LSAT), $NdGaO_3$, or $SrTiO_3$ substrates. Technically, this is feasible by either laser ablation [18-20], or by magnetron sputtering at high temperature [12]. It has been demonstrated that an increase in Hilbert damping in $SrIrO_3$/$La_{0.7}Sr_{0.3}MnO_3$ heterostructure is caused by spin current which flows across the interface [12,18,19]. Experimental studies of spin current characteristics under influence of spin pumping showed that the anisotropic magnetoresistance of $La_{0.7}Sr_{0.3}MnO_3$ also contributes to the total response along with the component, caused by spin current generation [8,12,13,18].

2. MATERIALS AND METHODS

Thin epitaxial films of strontium iridate $SrIrO_3$ (further, SIO3) and manganite $La_{0.7}Sr_{0.3}MnO_3$ (LSMO) with thicknesses of 10-50 nm were grown on single crystal (110)$NdGaO_3$ (NGO) substrates using radio frequency magnetron sputtering at substrate temperatures of 770-800°C in a mixture of Ar and O_2 gases at a total gas pressure of 0.3-0.5 mbar [12].

The crystal structure of obtained heterostructures was investigated by *X*-ray diffraction analysis and the transmission electron microscopy (TEM). **Fig. 1** shows a TEM image of cross section of the heterostructure, demonstrating the SIO3/LSMO interface and the interface of the LSMO film with the NGO substrate. We will describe the crystal lattice of SIO and LSMO as a distorted pseudo-cube with parameters a_{SIO} = 0.396 nm and a_{LSMO} = 0.389 nm, as the growth of heterostructure is realized by cube-on-cube mechanism with the following ratios: $SrIrO_3$||(001)$La_{0.7}Sr_{0.3}MnO_3$||(110) $NdGaO_3$, and [100] $SrIrO_3$||[100] $La_{0.7}Sr_{0.3}MnO_3$||[001] $NdGaO_3$ [12].

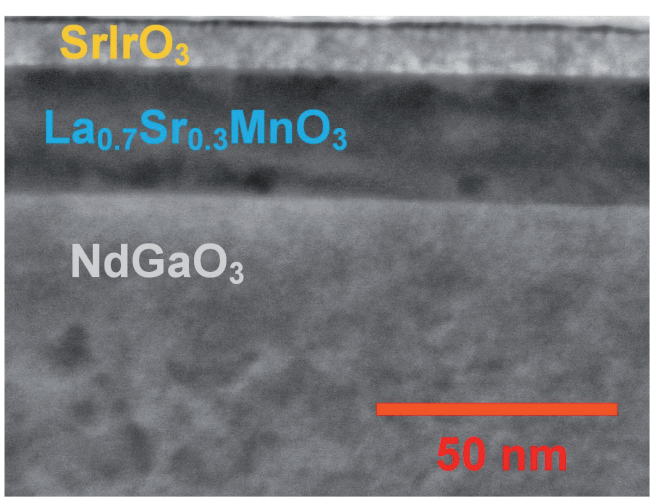

Fig. 1. *Cross section of $SrIrO_3$/$La_{0.7}Sr_{0.3}MnO_3$ heterostructure on $NdGaO_3$ substrate, obtained by transmission electron microscope. The additional Pt platinum film deposited for ion etching was removed.*

3. RESULTS AND DISCUSSION

In the SIO3/LSMO heterostructure, the paramagnetic SIO3 film plays role of a normal metal with strong SOI, while ferromagnetic LSMO is a half-metal with an almost 100% polarization at low temperatures.

In experiments with spin pumping at microwaves, the main decisive parameters are the spin diffusion length λ which characterizes spin current dissipation in N metal, and the spin-Hall angle θ_{SH} – the ratio of spin to charge currents at the N/F interface, and the spin mixing conductance $g^{\uparrow\downarrow}$, which is determined by the electron scattering matrix at N/F and characterizes the spin transfer transparency of angular magnetic momentum through the interface [4,5].

3.1. Spin current generation

At the FMR spin pumping, spin current j_S flows through the SIO3/LSMO interface, which is characterized by the spin mixing conductance $g^{\uparrow\downarrow}$, consisting of a real ($\mathrm{Re}\, g^{\uparrow\downarrow}$) and an imaginary part ($\mathrm{Im}\, g^{\uparrow\downarrow}$), as well by the amplitude of precession of magnetic moment m under influence of magnetic component of the microwave field [4,13]:

$$\mathrm{j_S} = \frac{h}{4\pi}\left(\mathrm{Re}\, g^{\uparrow\downarrow}\ \mathrm{m}\frac{\mathrm{dm}}{\mathrm{dt}} + \mathrm{Im}\, g^{\uparrow\downarrow}\frac{\mathrm{dm}}{\mathrm{dt}}\right). \qquad (1)$$

The spin current was recorded by measuring the voltage on a sample shaped ad s strip of SIO3/LSMO heterostructure grown on an NGO substrate with metal Pt contacts. To set the microwave magnetic field, the sample under the test was placed on a microstrip line, allowing to be carry out measurements in frequency band f = 2–20 GHz [10]. A constant magnetic H-field was set in the plane of the substrate and was directed perpendicular to the emerging charge current (along the Y axis), and the microwave magnetic field was excited by a short-circuited microstrip line with a microwave magnetic field component directed along the X axis. Precession of the magnetization of the LSMO film around the SIO3/LSMO strip induces a spin current perpendicular to the SIO3/LSMO interface (Z axis) and could be detected by voltage measurements due to ISHE (see inset in **Fig. 2**). The charge current j_Q is related to the spin current j_S through a dimensionless parameter – the spin Hall angle θ_{SH} [2,6]:

$$\vec{j}_Q = \theta_{SH}\frac{2e}{\hbar}\left[\vec{n}\times\vec{j}_S\right], \qquad (2)$$

where $\vec{n}$ is the unit vector of the spin momentum direction.

Fig. 2 shows the magnetic-field dependence of the voltage appeared on the SIO3/LSMO heterostructure under the influence of microwave field at frequency f = 2.3 GHz and power 20 mW at T = 300 K. It is seen that the sign of the response $V(H)$ is reversed when the direction of dc magnetic field is changed. This caused by the change in the direction of induced charge current due to direction reversal of vector $\vec{n}$, reversing the direction of dc magnetic field. In experiment, caused by parasitic microwave detection by Pt contacts some asymmetry of response amplitudes for opposite directions

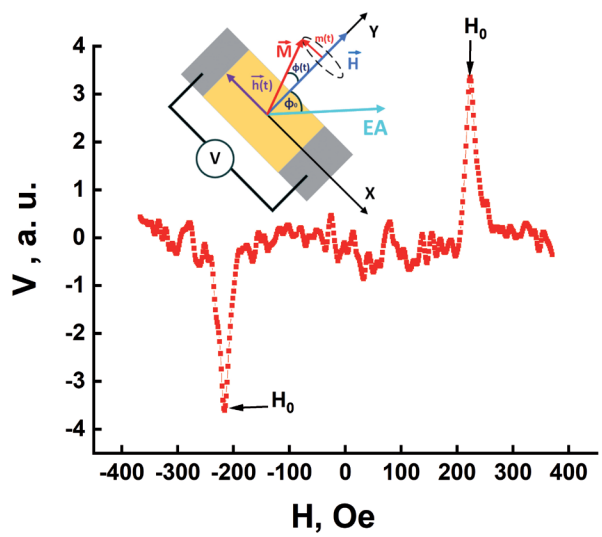

Fig. 2. *Magnetic-field dependence of the response of $SrIrO_3$/$La_{0.7}Sr_{0.3}MnO_3$ heterostructure to microwave field applied at frequency f = 2.3 GHz at T = 300 K with power of 30 mW. The inset shows the topology of the heterostructure indicating directions of microwave magnetic component h(t) and dc H magnetic field, as well as the direction of the charge current flow (registration of voltage V along the X axis) caused by the spin current.*

of *H*-field can be observed. An anisotropic magnetoresistance (AMR) response also contributes, which, however, under the certain conditions does not depend on direction of dc magnetic field [8,21].

Fig. 3 shows the voltage response caused by spin current at f = 2.3 GHz, T = 300 K, obtained from the half-difference of responses (Fig. 2) at opposite directions of *H*-field. The response shape is described well enough by the Lorentz function. The contribution caused by contacting phenomena and AMR was by an order in magnitude smaller, than amplitude of spin current response.

The flow of spin current through the interface causes an additional damping of spin precession. In experiment, this manifests itself in broadening of the FMR spectrum line , which is usually determined by the Hilbert spin damping coefficient α [4,11,22]. Parameters α and ΔH are coupled by a relation [23]: $\Delta H(f) = 4\alpha\pi f/\gamma + \Delta H_0$, where γ is the gyromagnetic ratio, and ΔH_0 – is broadening cased by magnetic inhomogeneity. Note, here we neglect the contributions of other damping sources (see, for example, [24]). The frequency-independent broadening ΔH_0 = 6±1 Oe is small and determined by the magnetic inhomogeneity of the LSMO film in the heterostructure. For LSMO films we get α_{LSMO} = (2.0±0.2)·10^{-4} and damping increases in heterostructure SIO3/LSMO $\alpha_{SIO/LSMO}$ = (6.7±0.8)·10^{-4}. The increase in Hilbert damping after deposition of SIO3 film makes it possible to estimate the real part of the spin mixing conductance Re$g^{\uparrow\downarrow}$ [4,21,25]. For LSMO magnetization M = 370 Oe and the thickness of the LSMO film d_{LSMO} = 30 nm, we obtain Re$g^{\uparrow\downarrow}$ = (3.5±0.5)·10^{18} m^{-2}. Note, that the obtained value coincides in order of magnitude with Re$g^{\uparrow\downarrow}$ = 1.3·10^{18} m^{-2}, determined in [19]. Changing thin film thickness of $SrIrO_3$ in SIO3/LSMO heterostructure from 1.5 nm to 12 nm value of Re$g^{\uparrow\downarrow}$ is changed from 0.5·10^{19} m^{-2} to 3.6·10^{19} m^{-2} [18].

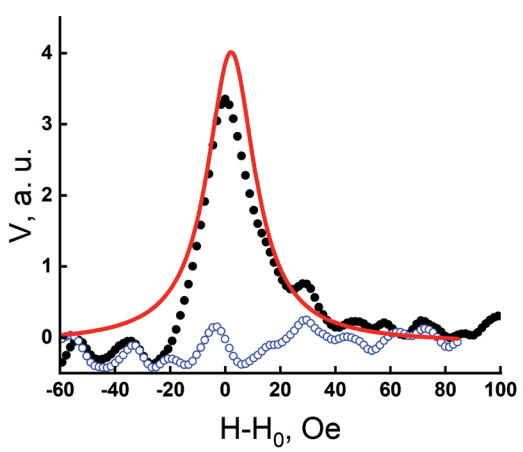

Fig. 3. *Voltage response induced by spin current at FMR pumping frequency f = 2.3 GHz, T = 300 K, obtained from the half difference of peaks at opposite directions of dc magnetic field. Filled circles are experimental, solid line is the Lorentz line approximation. Empty circles - response caused by parasitic contact phenomena and anisotropic magnetoresistance (half-sum of peaks at opposite directions of magnetic field).*

According to the theory based on the spin interaction between localized and conducting electrons the spin mixing conductance Re$g^{\uparrow\downarrow}$ is determined by resistivity ϱ_{SIO} and spin diffusion length λ_{SIO} of the normal metal with SOI, in our case SIO3 film [25]:

$$\mathrm{Re}g^{\uparrow\downarrow} \approx (h/e^2)/(\varrho_{SIO}\lambda_{SIO}). \quad (3)$$

Taking $h/e^2 \approx 25.8$ *kΩ* , for λ_{SIO} = 1 nm [19] and ϱ_{SIO} = 3·10^{-4} *Ω* cm [12] from relation (4)

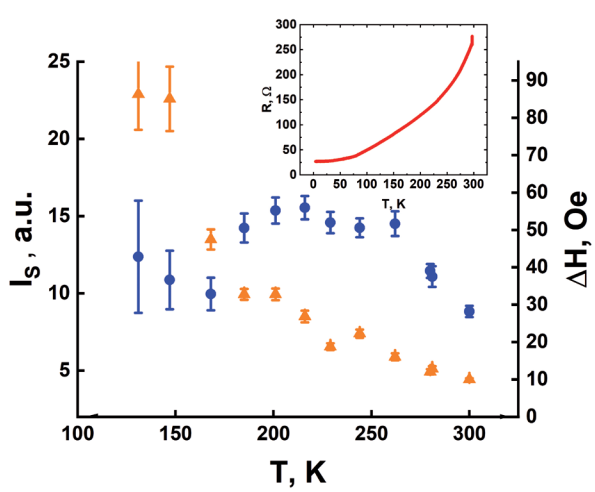

Fig. 4. *Temperature dependences of spin current amplitude (filled circles) and line-widths (filled triangles). The spin current value is obtained by dividing the voltage response by the resistance of heterostructure. Inset: temperature dependence of heterostructure's resistance at H = 0.*

we obtain $Reg^{\uparrow\downarrow} \approx 8.6 \cdot 10^{18}$ m^{-2}. The obtained value is consistent in order of magnitude with the experimental data for 3*d* transition metals, and for metallic ferromagnets Co, Ni, Fe the parameter $Reg^{\uparrow\downarrow}$ is in the range $6 \cdot 10^{18}$-$8 \cdot 10^{20}$ m^{-2} [25,26], although relation (3) is just a qualitative estimate of $Reg^{\uparrow\downarrow}$ and does not take into account the influence of spin-orbit interaction.

Assuming that the deviation of the $H_0(f)$ dependence for SIO3/LSMO heterostructure from $H_0(f)$ of the LSMO film can be described by a change in gyromagnetic ratio γ and attributed to a presence of an imaginary part of the spin mixing conductance, we obtain a value for significantly higher than estimated for ferromagnetic structures with Pt [4,22].

Closer to realistic experimental conditions, on our opinion, is $Img^{\uparrow\downarrow}$ 10^{19} m^{-2}, obtained taking into account the error of $H_0(f)$ function measurement. As shown in works [12,22], indeed, value of $Img^{\uparrow\downarrow}$ is comparable to the value of $Reg^{\uparrow\downarrow}$. Moreover, measurements of Hall magnetoresistance for Pt/EuS [27] and W/EuO [28] structures showed that $Img^{\uparrow\downarrow}$ exceeds $Reg^{\uparrow\downarrow}$ by a factor of 3 and 10 times, respectively. Note, the appearance of magnetization in the direction perpendicular to the plane, for example as in the case of superlattice made from SIO3/LSMO heterostructures may play a significant role [17].

Fig. 4 shows the temperature dependence of the spin current amplitude and response linewidth of the heterostructure. The spin current amplitude is obtained from response voltage division by the resistance of the heterostructure, shown in the inset to Fig. 4. It is seen that an increase of spin current observed with decreasing the temperature for the Pt/LSMO heterostructure [8] is not observed in our case, which is probably caused by the presence of a conducting layer at the SIO3/LSMO interface [13].

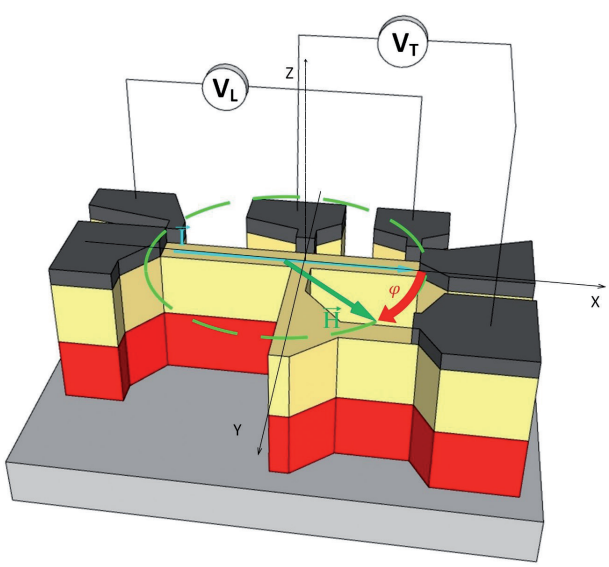

Fig. 5. *Schematic 3D image of $SrIrO_3/La_{0.7}Sr_{0.3}MnO_3$ heterostructure on (110)$NdGaO_3$ substrate with Pt contact pads. The current I is set along the X axis, the angle φ between the magnetic field H and the current I was varied by rotating the sample in the X-Y plane.*

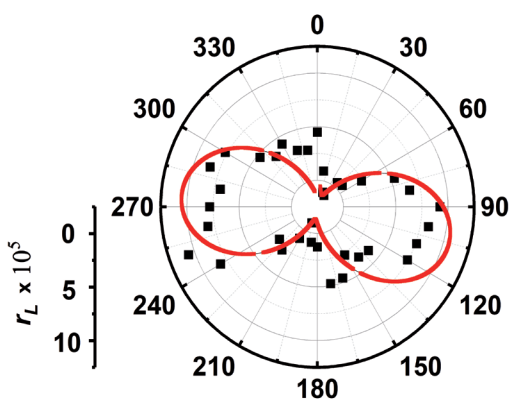

a

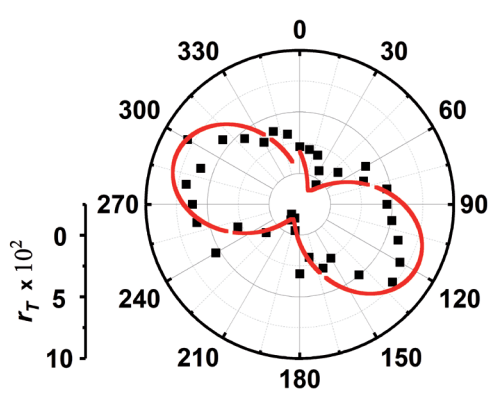

b

Fig. 6. *Angular dependences of normalized values of magnetoresistance of heterostructure $r_L(T)$ (squares) and approximation by sinusoidal dependence (solid line) in polar coordinates, taken at the field H = 100 Oe at T = 300 K. (a) transverse magnetoresistance, (b) longitudinal. The scale of magnetoresistance variation is shown on the left.*

3.2. Spin current detection using inverse spin Hall effect

The inverse spin Hall effect (ISHE) is used to detect the spin current [1,5]. In this case, the ratio of spin and charge currents is determined by a dimensionless parameter – spin Hall angle θ_{SH} (2) [2,6].

For determination the θ_{SH} value, the Hall geometry of the SIO3/LSMO heterostructure shown in **Fig. 5** and a 4-point measurement scheme was used. A constant magnetic field H was set in the plane of the SIO3/LSMO interface of heterostructure. The measured voltages were V_L, proportional to the longitudinal magnetoresistance, and V_T, proportional to the transverse (planar) Hall magnetoresistance. Along the X direction (see Fig. 5), a current I = 0.5 mA at frequency F = 1.1 kHz was set and a lock-in amplifier with high-sensitivity was used for voltage measurement. The substrate with the sample was rotated around the normal to the substrate in order to change the angle φ between the magnetic field H and the current I. The longitudinal magnetoresistance was determined from $R_L = V_L/I$, and the transverse magnetoresistance by $R_T = V_T/I$.

Magnetic-field dependences in normalized units of the change in magnetoresistance $r_{L(T)} = \Delta R_{L(T)}/R_0$ (longitudinal ΔR_L, and transverse ΔR_T) of SIO3/LSMO heterostructure, where $\Delta R_{L(T)} = R_{L(T)} - R_0$ (R_0 – magnetoresistance at $H = 0$) vs. angle φ between magnetic field H and current I were recorded. The obtained values were compared with magnetoresistance measurements for LSMO films, as well as for structures with a platinum film deposited on top of an epitaxial LSMO film on a substrate (Pt/LSMO). The measured longitudinal magnetoresistance $r_L(\varphi)$ contains in addition to the spin longitudinal magnetoresistance r_{LS} also a contribution from the anisotropic magnetoresistance (AMR) of the ferromagnetic LSMO film $r_A = R_A/R_0$. For the case of transverse magnetoresistance $r_T(\varphi)$ contains also a component of the planar Hall effect magnetoresistance.

Fig. 6a shows the angular dependence of the longitudinal magnetoresistance $r_L(\varphi)$ of the SIO3/LSMO heterostructure in polar coordinates. The dependence of $r_L(\varphi)$ observed in the experiment is a parallel connection of r_{LS} and r_A. In this case, the angular dependence of AMR is described by the function $r_A \cos 2\varphi$, which looks like a dependence of spin magnetoresistance of the SIO3/LSMO heterostructure [6]:

$$r_{LS} = r_1 \cos^2 \varphi, \quad (4)$$

where

$$r_1 = \theta_{SH}^2 \frac{\lambda_{SIO}}{d_{SIO}} \mathrm{Re} \frac{2\lambda_{SIO}\rho_{SIO}(\mathrm{ReG}^{\uparrow\downarrow} + i\,\mathrm{ImG}^{\uparrow\downarrow})}{1 + 2\lambda_{SIO}\rho_{SIO}(\mathrm{ReG}^{\uparrow\downarrow} + i\mathrm{ImG}^{\uparrow\downarrow})}. \quad (5)$$

$\mathrm{ReG}^{\uparrow\downarrow} = \mathrm{Reg}^{\uparrow\downarrow} e^2/h$, $\mathrm{ImG}^{\uparrow\downarrow} = \mathrm{Img}^{\uparrow\downarrow} e^2/h$, it is assumed that the spin diffusion length λ_{SIO} is much smaller than the SIO3 film thickness d_{SIO}. When current I flows longitudinally (along the X direction) we obtain a sinusoidal dependence $r_L(\varphi)$ (Fig. 6*a*). The phase shift in $r_L(\varphi)$ is caused by the difference between the coordinate of the substrate edge, from which the angle φ is counted, and the direction of the LSMO film magnetization easy axis, which is given by the crystallographic direction of the [001]$NdGaO_3$ substrate on which the LSMO film was epitaxially grown [12]. Using the values of SIO3 film resistivity $\varrho_{SIO} = 3 \cdot 10^{-4}$ Ω cm [12] and λ_{SIO} = 1

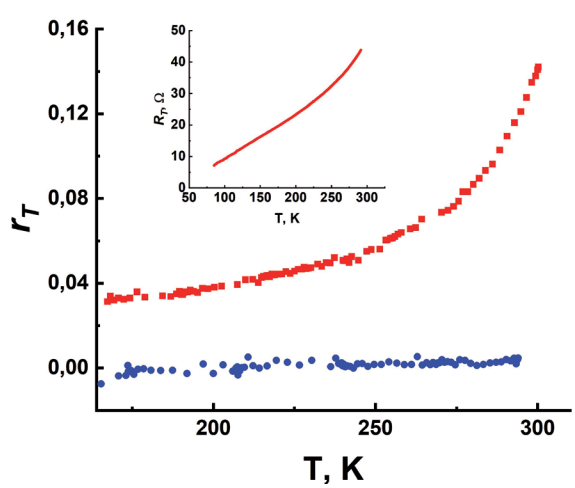

Fig. 7. *Temperature dependence of transverse (Hall) magnetoresistance r_T. Curve (1) corresponds to the angle φ = 210°, at which r_T is maximum, curve (2) was taken at the minimum value of r_T (φ = 275°). The inset shows the temperature dependence of the transverse (Hall) resistance at H = 0.*

nm [19] obtained at room temperature and the data for $Reg^{\uparrow\downarrow}$ и $Img^{\uparrow\downarrow}$ from the Part 3.1. of this paper, for thicknesses d_{SIO} = 10 nm and d_{LSMO} = 30 nm from amplitudes of magnetoresistance $r_L(\varphi)$ using eq. (4) and (5) we obtain $\theta_{SH} = 0.03\pm0.01$ for spin-Hall angle. Obtained value is an order of magnitude smaller than for the transverse case (Fig. 6*b*), but is about 4 times larger than the spin Hall angle for c Pt heterostructures [3,6,8].

Fig. 6*b* shows the angular dependence of the transverse magnetoresistance $r_T(\varphi)$ in polar coordinates of the SIO3/LSMO heterostructure which, in the general case, is the sum of the contributions from the spin-Hall magnetoresistance r_H and the contribution from the out-of-plane magnetoresistance r_2 [6].

$$r_{TS} = \frac{r_1}{2}\sin 2\varphi + r_2 \cos\theta, \qquad (6)$$

where θ is the angle between the current and magnetization along the Z axis perpendicular to the substrate plane (not shown in Fig. 5). The obtained values of r_T turn out are by an order of magnitude larger than in the case of the longitudinal magnetoresistance r_L even considering existence only the first term in (6) at $\theta = \pi/2$. As a result, from the data from $r_T(\varphi)$ we obtain $\theta_{SH} = 0.35\pm0.05$ for the SIO3/LSMO heterostructure. Thus, from the transverse magnetoresistance measurements, we obtained a value of θ_{SH} about 10 times larger than that from the longitudinal magnetoresistance, which, likely, caused by shunting of the longitudinal AMR magnetoresistance of the LSMO film [13]. Note, $\theta_{SH} \approx 0.3$ was obtained in SIO3/LSMO heterostructures [11,16] by other methods. The second term dependent on the imaginary part of the complex spin mixing conductance [6] in eq. (6) arises due to the magnetization directed perpendicular to the substrate plane and can cause an increase in magnetoresistance, which was observed in SIO3/LSMO superlattices [17]. High values of the spin Hall angle in structures with SIO3 films were reported earlier: θ_{SH} = 0.76 for Py/$SrIrO_3$ [15] and θ_{SH} = 1.1 for $SrIrO_3$/$Co_{1-x}Tb_x$ [29]. In order of magnitude, these values are close to θ_{SH}, observed in structures with topological insulators [30].

When the SIO3/LSMO heterostructure was cooled down to liquid nitrogen temperature T=77 K, the magnetoresistance value decreased. **Fig. 7** shows the temperature dependence of the normalized transverse value of r_T for two cases of $r_T(\varphi)$ at fixed values of the angle φ: when r_T is maximal (φ = 210º) and minimal (φ = 275º) at T = 300 K. At low temperatures (T < 150 K) the measurement error (not shown in Fig. 7) no longer allowed to extract reliable data. At T = 77 K, neither transverse, nor longitudinal magnetoresistance could be detected. The temperature dependence of the transverse resistivity of the SIO3/LSMO heterostructure R_T, taken at H = 0 is shown in the inset to Fig. 7. In general, the nature of the temperature dependence of $R_T(T)$ is similar to the temperature dependence of the planar Hall resistance $r_T(T)$. It is known that the magnetization M of an LSMO film increases with decreasing temperature, but relations (4)–(6) [6] do not imply a change in the Hall magnetoresistance with temperature. Note, that the temperature dependences of the characteristics of magnetoresistance, spin diffusion length, and spin Hall angle were considered in [30,31] for structures different from those considered in this work, as well as for the case of spin moment changes in SIO3/LSMO [20,32] under the influence of current pulses. Note also, that the observed increase in spin current with decreasing temperature for Pt/LSMO [8] is not observed in our case, which is probably due to the influence of the conducting layer at the SIO3/LSMO interface [12]. Note, that the changes of magnetoresistance with temperature can be caused by the temperature dependences of $Reg^{\uparrow\downarrow}$ and $Img^{\uparrow\downarrow}$. Varying the numerical value of the ratio $Img^{\uparrow\downarrow}/Reg^{\uparrow\downarrow}$ in (5) does not lead to a noticeable change in the parameter r_1, but can affect parameter r_2 in the case of the occurrence of out-of-plane magnetization in *F*-layer.

4. CONCLUSION

It is shown experimentally that under applied microwaves the spin current response in $SrIrO_3/La_{0.7}Sr_{0.3}MnO_3$ heterostructure exceeds the response caused by contributions due to parasitic detection at contacts and anisotropic magnetoresistance by an order in magnitude. It is shown that the imaginary part of the spin mixing conductance in $SrIrO_3/La_{0.7}Sr_{0.3}MnO_3$ interface turns out, by an order of magnitude, is equal to its real part. It was found out that the amplitude of the angular dependence of the transverse magnetoresistance significantly exceeds the amplitude of the longitudinal one, which is, most likely, affected by the shunting effect of the anisotropic magnetoresistance of the film $La_{0.7}Sr_{0.3}MnO_3$ and by the conducting layer at the interface of the heterostructure $SrIrO_3/La_{0.7}Sr_{0.3}MnO_3$. The spin-Hall angle (the ratio of spin and charge currents) determined from measurements of the longitudinal spin magnetoresistance was by an order of magnitude smaller than for the transverse (Hall) magnetoresistance, which is caused by the presence of a conducting layer at the heterostructure interface. As the temperature decreases below room temperature, we did not find any significant increase in spin current value, both from the direct detection of the spin current due to the inverse spin-Hall effect, and from the temperature dependence of the spin magnetoresistance.

REFERENCES

1. Dyakonov MI, and Perel VI. On possibility of orientation of spin by current. *JETP Lett.*, 1971, 13:467-469.
2. Saitoh E, Ueda M, Miyajima H, and Tatara S. Conversion of spin current into charge current at room temperature: Inverse spin-Hall effect. *Appl. Phys. Let.*, 2006, 88(18):182509-1-3.
3. Mosendz O, Vlaminck V, Pearson JE, Fradin FY, Bauer WGE, Bader SD, and Hoffmann A. Detection and quantification of inverse spin Hall effect from spin pumping in permalloy/normal metal bilayers. *Phys. Rev. B*, 2010, 82(21):214403-1-9.
4. Tserkovnyak Y, Brataas A, Bauer GEW. Enhanced Gilbert damping in thin ferromagnetic films. *Phys Rev. Lett.,* 2002, 88(11):117601-1-4.
5. Sinova J, Valenzuela SO, Wunderlich J, Back CH, Jungwirth T. Spin Hall effects. *Rev.Mod. Phys.*, 2015, 87(4):1213-1259.
6. Chen YT, Takahashi S, Nakayama H, Althammer M, Goennenwein ST, Saitoh E, Bauer GE. Theory of spin Hall magnetoresistance (SMR) and related phenomena. *J of Physics: Condensed Matter,* 2016, 28(10):103004-1-15.
7. Althammer M, Meyer S, Nakayama H, Schreier M, Altmannshofer S, Weiler M, Huebl H, Geprägs S, Opel M, Gross R, Meier D, Klewe C, Kuschel T, Schmalhorst J-M, Reiss G, Shen L, Gupta A, Chen Y-T, Bauer GEW, Saitoh E, Goennenwein ST. Quantitative study of the spin Hall magnetoresistance in ferromagnetic insulator/normal metal hybrids. *Phys. Rev. B,* 2016, 87(22):224401-1-15.
8. Azevedo A, Vilela-Leão LH, Rodríguez-Suárez RL, Santos AL, Rezende SM. Spin pumping and anisotropic magnetoresistance voltages in magnetic bilayers: Theory and experiment. *Phys. Rev. B,* 2011, 83(14):144402-1-6.
9. Sandweg CW, Kajiwara Y, Ando K, Saitoh E, Hillebrands B. Enhancement of the spin pumping efficiency by spin wave mode selection. *Appl. Phys. Lett.*, 2010, 97(25):252504-1-4.
10. Ovsyannikov GA, Constantinian KY, Stankevich KL, Shaikhulov TA, Klimov AA. Spin current and spin waves at a platinum/yttrium iron garnet interface: impact of microwave power and temperature. *J. of Physics D: Applied Physics,* 2021, 54(36):365002-1-11.
11. Nan T, Emori S, Boone CT, Wang X, Oxholm TM, Jones JG, Howe BM, Brown GJ, Sun NX. Comparison of spin-orbit

torques and spin pumping across NiFe/Pt and NiFe/Cu/Pt interfaces. *Phys. Rev.B,* 2015, 91(21):214416-1-9.
12. Ovsyannikov GA, Shaikhulov TA, Stankevich KL, Khaydukov Y, Andreev NV. Magnetism at an iridate/manganite interface: Influence of strong spin-orbit interaction. *Phys. Rev. B*, 2020, 102(14):144401-1-11.
13. Ovsyannikov GA, Constantinian KY, Shmakov VA, Klimov AL, Kalachev EA, Shadrin AV, Andreev NV, Milovich FO, Orlov AP, Lega PV. Spin mixing conductance and spin magnetoresistance of the iridate/manganite interface. *Phys. Rev. B,* 2023, 107(14):144419-1-12.
14. Qi XL, Zhang SC. Topological insulators and superconductors. *Rev. Mod. Phys.,* 2011, 83(4):1057-1103.
15. Nan T, Anderson TJ, Gibbons J, Hwang K, Campbell N, Zhou H, Dong YQ, Kim GY, Shao DF, Paudel TR, Reynolds N, Wang XJ, Sun NX, Tsymbal EY, Choi SY, Rzchowski MS, Kim YB, Eom CB. *Proc. Natl. Acad. Sci. USA,* 2019, 116(33):16186-16191.
16. Everhardt AS, Mahendra DC, Huang X, Sayed S, Gosavi TA, Tang Y, Lin CC, Manipatruni S, Young IA, Datta S, Wang J-P, Ramesh R. Tunable charge to spin conversion in strontium iridate thin films. *Phys. Rev. Materials*, 2019, 3(5):051201-1-18.
17. Yi D, Liu J, Hsu SL, Zhang L, Choi Y, Kim JW, Chen Z, Clarkson JD, Serrao CR, Arenholz E, Ryan PJ, Xu H, Birgeneau RJ, RameshR. Atomic-scale control of magnetic anisotropy via novel spin–orbit coupling effect in La2/3Sr1/3MnO3/SrIrO3 superlattices. *Proceedings of the National Academy of Sciences USA*, 2016, 113(23):6397-6402.
18. Huang X, Sayed S, Mittelstaedt J, Susarla S, Karimeddiny S, Caretta L, Zhang H, Stoica VA, Gosavi T, Mahfouzi F, Sun Q, Ercius P, Kioussis N, Salahuddin S, Ralph DC, Ramesh R. Novel Spin–Orbit Torque Generation at Room Temperature in an All-Oxide Epitaxial $La_{0.7}Sr_{0.3}MnO_3/SrIrO_3$ System. *Advanced Materials,* 2021, 33(24):2008269-1-7.
19. Crossley S, Swartz AG, Nishio K, Hikita Y, Hwang HY. All-oxide ferromagnetic resonance and spin pumping with $SrIrO_3$. *Physical Review B,* 2019, 100(11):115163-1-7.
20. Liu L, Zhou G, Shu X, Li C, Lin W, Ren L, Zhou C, Zhao T, Guo R, Xie Q, Wang H, Zhou J, Yang P, Pennycook SJ, Xu X, Chen J. Room-temperature spin-orbit torque switching in a manganite-based heterostructure. *Phys. Rev. B*, 2022, 105(14):144419-1-11.
21. Atsarkin VA, Borisenko IV, Demidov VV, Shaikhulov TA. Temperature dependence of pure spin current and spin-mixing conductance in the ferromagnetic—normal metal structure. *Journal of Physics D: Applied Physics*, 2018, 51(24):245002-245002.
22. Zwierzycki M, Tserkovnyak Y, Kelly PJ, Brataas A, Bauer GE. First-principles study of magnetization relaxation enhancement and spin transfer in thin magnetic films. *Phys. Rev. B*, 2005, 71(6):064420-1-11.
23. Yang F, Hammel PC. FMR-driven spin pumping in $Y_3Fe_5O_{12}$-based structures. *Journal Physics D: Applied Physics,* 2018, 51(25):253001-1-9.
24. Shaikhulov TA, Ovsyannikov GA. Attenuation of spin precession in manganite/normal metal heterostructures. *Physics of the Solid State,* 2018, 60:2231-2236.
25. Dubowik J, Graczyk P, Krysztofik A, Głowiński H, Coy E, Załęski K, Gościańska I. Non-Negligible Imaginary Part of the Spin-Mixing Conductance and its Impact on Magnetization Dynamics in Heavy-Metal–Ferromagnet Bilayers. *Physical Review Applied,* 2020, 13(5):054011-1-13.
26. Czeschka FD, Dreher L, Brandt MS, Weiler M, Althammer M, Imort IM, Reiss G, Thomas A, Schoch W, Limmer W, Huebl H, Goennenwein ST. Scaling behavior of the spin pumping effect in ferromagnet-platinum bilayers. *Phys. Rev. Lett.*, 2011, 107(4):046601-1-4.

27. Gomez-Perez JM, Zhang XP, Calavalle F, Ilyn M, González-Orellana C, Gobbi M,Rogero C, Chuvilin A, Golovach VN, Hueso LE, Bergeret FS, Casanova F. Strong interfacial exchange field in a heavy metal/ferromagnetic insulator system determined by spin Hall magnetoresistance. *Nano Letters*, 2020, 20(9):6815-6823.
28. Rosenberger P, Opel M, Geprägs S, Huebl H, Gross R, Müller M, Althammer M. Quantifying the spin mixing conductance of EuO/W heterostructures by spin Hall magnetoresistance experiments. *Applied Physics Letters,* 2021, 118(19):192401-1-5.
29. Wang H, Meng KY, Zhang P, Hou JT, Finley J, Han J, Yang F, Liu L. Large spin-orbit torque observed in epitaxial $SrIrO_3$ thin films. *Applied Physics Letters,* 2019, 114, 23:232406-1-5.
30. Yi D, Liu J, Hsu SL, Zhang L, Choi Y, Kim JW, Chen Z, Clarkson JD, Serrao CR, Arenholz E, Ryan PJ, Xu H, Birgeneau RJ, Ramesh R. Atomic-scale control of magnetic anisotropy via novel spin–orbit coupling effect in $La_{2/3}Sr_{1/3}MnO_3/SrIrO_3$ superlattices. *Proceedings of the National Academy of Sciences*, 2016, 113(23):6397-6402.
31. Marmion SR, Ali M, McLaren M, Williams DA, Hickey BJ. Temperature dependence of spin Hall magnetoresistance in thin YIG/Pt films. *Phys. Rev. B*, 2014, 89(22):220404-1-5.
32. Wang Y, Deorani P, Qiu X, Kwon JH, Yang H. Determination of intrinsic spin Hall angle in Pt. *Applied Physics Letters,* 2014, 105(15):152412-1-4.
33. Yi D, Amari H, Balakrishnan PP, Klewe C, Shafer P, Browning N, Suzuki Y. Enhanced interface-driven perpendicular magnetic anisotropy by symmetry control in oxide superlattices. *Physical Review Applied,* 2021, 15(2):024001-1-9.